



THE UNIVERSITY *of* EDINBURGH

Edinburgh Research Explorer

Live imaging and analysis of cilia and cell cycle dynamics with the Arl13bCerulean-Fucci2a biosensor and Fucci Tools

Citation for published version:

Van Kerckvoorde, M, Ford, MJ, Yeyati, P, Mill, P & Mort, R 2021, Live imaging and analysis of cilia and cell cycle dynamics with the Arl13bCerulean-Fucci2a biosensor and Fucci Tools. in *Cell Cycle Oscillators : Methods in Molecular Biology*. vol. II, Springer. https://doi.org/10.1007/978-1-0716-1538-6_21

Digital Object Identifier (DOI):

https://doi.org/10.1007/978-1-0716-1538-6_21

Link:

[Link to publication record in Edinburgh Research Explorer](#)

Document Version:

Peer reviewed version

Published In:

Cell Cycle Oscillators

General rights

Copyright for the publications made accessible via the Edinburgh Research Explorer is retained by the author(s) and / or other copyright owners and it is a condition of accessing these publications that users recognise and abide by the legal requirements associated with these rights.

Take down policy

The University of Edinburgh has made every reasonable effort to ensure that Edinburgh Research Explorer content complies with UK legislation. If you believe that the public display of this file breaches copyright please contact openaccess@ed.ac.uk providing details, and we will remove access to the work immediately and investigate your claim.



Live imaging and analysis of cilia and cell cycle dynamics with the Arl13bCerulean-Fucci2a biosensor and Fucci Tools

Melinda Van Kerckvoorde¹, Matthew J. Ford², Patricia L. Yeyati³, Pleasantine Mill^{3*}, and Richard
5 L. Mort^{1*}

1. Division of Biomedical and Life Sciences, Faculty of Health and Medicine, Furness Building,
Lancaster University, Bailrigg, Lancaster, LA1 4YG, UK

2. Goodman Cancer Research Centre, Department of Human Genetics, McGill University,
10 Montreal, Quebec, H3A 1A3, Canada

3. MRC Human Genetics Unit, MRC Institute of Genetics & Molecular Medicine, University of
Edinburgh, Western General Hospital, Edinburgh, EH4 2XU, UK

*Correspondence: r.mort@lancaster.ac.uk, pleasantine.mill@igmm.ed.ac.uk

15

Abstract

20 The cell and cilia cycles are inextricably linked through the dual functions of the centrioles at both the basal body of cilia and at mitotic centrosomes. How cilia assembly and disassembly, either through slow resorption or rapid deciliation, are coordinated with cell cycle progression remains unclear in many cell types and developmental paradigms. Moreover, little is known about how additional cilia parameters including changes in ciliary length or frequency of distal tip shedding change with cell cycle stage. In order to explore these questions, we have

25 developed the Arl13bCerulean-Fucci2a tricistronic cilia and cell cycle biosensor (Ford et al 2018). This reporter allowed us to document the heterogeneity in ciliary behaviors during the cell cycle at a population level. Without the need for external stimuli, it revealed that in several cell types and in the developing embryo cilia persist beyond the G1/S checkpoint. Here, we describe the generation of stable cell lines expressing Arl13bCerulean-Fucci2a and open-source

30 software to aid morphometric profiling of the primary cilium with cell cycle phases, including changes in cilium length. This resource will allow the investigation of multiple morphometric questions relating to cilia and cell cycle biology.

Key words: cell cycle, cilia, ImageJ, image analysis, live cell imaging, Fucci2A, biosensor,

35 morphometrics, cell division, ciliogenesis.

1. Introduction

Cilia are small microtubule-based protrusions projecting from the surface of most mammalian cell types. Akin to cellular 'antennae', primary cilia play critical roles in sensing and eliciting cellular responses to environmental and developmental signals, from embryogenesis through to adult tissue homeostasis. These specialized signaling 'organelles' are compartmentalized with a distinct protein and lipid composition maintained by dedicated selective trafficking modules and structural elements (Garcia-Gonzalo and Reiter 2017). Defects in cilia structure and/or function result in a group of genetic disorders termed the ciliopathies, where the alterations in gross cilia morphology observed in patient cells have been proposed to underlie the clinical phenotypes (Reiter and Leroux 2017). However, it is also possible that biochemical changes in the cilia compartment may affect cilia function, at a transient stage in cell cycle progression or without altering length or stability at all. Therefore, better tools are required to resolve cilia dynamics in order to understand gene function.

Moreover, cilia are not static structures. The assembly, elongation and resorption of the ciliary axoneme is regulated by cytoskeletal dynamics that define centrosome positioning across the cell cycle (Bernabé-Rubio and Alonso 2017). Ciliogenesis is a highly regulated process that is led by the mother centriole, destined to become the basal body of the nascent cilium. The basal body acts as a cilia microtubule organizing center (MTOC) nucleating the positive end of the microtubules and orientating them out of the cell into the soon-to-be ciliary tip. Subsequent elongation of cilia requires anterograde and retrograde intraflagellar transport (IFT) along the axoneme and is critical for its function (Ishikawa and Marshall 2017). In order to divide, cells must dismantle their cilia to free up the centrioles and form the mitotic spindle. How this process occurs in asynchronous populations like the rapidly growing embryo, versus synchronized cells in culture which re-enter the cell cycle following serum addition, remains unclear (Wang and Dynlacht 2018). In contrast to synchronized culture experiments, where there are two distinct phases of cilia disassembly (Tucker et al 1979; Pugacheva et al 2007), the

precise timing of cilia assembly and disassembly in relation to the cell cycle in actively cycling cells is still ill-defined. We and others have previously shown that whilst the initial cilia
65 assembly time is more variable in terms of kinetics, cilia disassembly during interphase occurs in a tight window ahead of mitosis across the asynchronous population (Anderson and Stearns 2009; Ford et al 2018). In an actin-dependent process they term 'decapitation', Phua et al demonstrated that the release of vesicles from the distal ciliary tip in response to serum was required for ciliary disassembly and cell cycle re-entry, including from quiescence (Phua et al
70 2017). Recent work by Mirvis et al (Mirvis et al 2019) showed that in IMCD3 cells a rapid deciliation which involved shedding of the ciliary axoneme and membrane was the predominant mode of deciliation, one dependent on katanin activity, in response to serum. There is much to be learned about the heterogeneity in cell behaviors exhibited during cilia disassembly in asynchronous populations. For example, how does cilia length change during
75 cell cycle progression? Does decapitation occur at specific cell cycle ? And do cilia disassemble in a cell-type and context-dependent manner?

To better understand these processes, we used Fucci2a (Fluorescent Ubiquitination-based Cell
Cycle Indicator 2a), a multicistronic construct that encodes two cell cycle biosensors fused using the *Thosea asigna* virus 2A (T2A) self-cleaving peptide sequence (Mort et al 2014). hCdt1-
80 mCherry incorporates a truncated form of human CDT1 (amino acids 30-120) fused to the mCherry fluorescent protein, whereas hGem-mVenus includes a truncated form of human Geminin (amino acids 1-110) fused to mVenus. Fucci2a allows discrimination between cell cycle phases in live cells using imaging of mCherry and mVenus abundance (Mort et al 2014). CDT1 abundance peaks during the G1 cell cycle phase in order to recruit the replicative DNA helicase,
85 whereas Geminin is stable from S until M phase as an inhibitor of CDT1 ensuring that DNA replication happens only once per cell cycle (Sakaue-Sawano et al 2008). Hence, the advantage of co-expressing these fluorescent markers is the ability to image their reciprocal abundance in proliferating cells without artificially perturbing cell cycle progression. To this construct we

added a marker to image the primary cilium across the different cell cycle oscillations, by fusing
90 the ciliary GTPase ARL3B to the fluorescent protein mCerulean (Ford et al 2018). This fusion
protein was then fused with Fucci2a using the *porcine teschovirus-1* P2A self-cleaving peptide
sequence (**Fig. 1A**). We demonstrated in asynchronously cycling NIH-3T3 cells that cilia
assemble across a wide window of cell cycle stages in interphase, and that these cilia persist just
prior to mitosis (Ford et al 2018). Further comparisons tracking the fate of daughter cells
95 revealed that daughter cells from ciliated mother cells assemble their primary cilia faster than
from non-ciliated mothers and that one daughter cell tends to initiate ciliogenesis earlier than
the other, confirming previous studies (Paridaen et al 2013; Ford et al 2018). We also showed
with the development of a Cre-inducible *R26Arl13b-Fucci2aR* reporter mouse that we could
generate high-resolution images enabling tracking of the cell cycle stage and ciliation state of
100 individual cells in culture and in all tissues examined, both embryonic and adult (Ford et al
2018).

Here, we present detailed methods and novel analytical tools to streamline monitoring cilia
behaviors across cell cycle transitions. We describe the generation of stable cell lines expressing
Arl13bCerulean-Fucci2a, their live imaging by confocal microscopy and the simultaneous
105 analysis of cell cycle and cilia dynamics using Fucci Tools software to generate high quality
tracking data and multifactorial plots of cell cycle and cilia cycle kinetics.

2. Materials

Prepare all solutions using ultrapure water and store at room temperature (unless
indicated otherwise).

110 2.1. Cell culture

1. Mouse Flp-In™-3T3 cells (ThermoFisher, cat. no. **R76107**) or *Arl13bCerulean-Fucci2a* 3T3
cells (Ford et al 2018 - Riken BRC accession #RCB5029) (*see Note 1*).

2. Culture medium: Dulbecco's Modified Eagle's Medium (DMEM), 10% Fetal bovine serum (FBS), 1% Penicillin/Streptomycin, 25 mM D-Glucose, 4 mM L-glutamine, 1 mM sodium pyruvate.
3. Imaging medium: Phenol red-free Dulbecco's Modified Eagle's Medium (DMEM), 10% Fetal bovine serum (FBS), 1% Penicillin/Streptomycin, 25 mM D-Glucose, 4 mM L-glutamine, 1 mM sodium pyruvate
4. Freezing medium: 45 mL culture medium, 5 mL Dimethyl sulfoxide (DMSO).
5. Opti-MEM (ThermoFisher, cat. no. 31985062).
6. Phosphate Buffered Saline (1x PBS).
7. 0.25% Trypsin-EDTA (1x).
8. Zeocin: 100 mg/mL, store at -20°C.
9. Hygromycin B: 50 mg/mL. store at 4°C.
10. 1 x TE buffer: 10 mM Tris-HCl, 1 mM EDTA.
11. 15 ml sterile, conical tubes.
12. 1.5 ml sterile, tubes.
13. 2 ml cryovials.
14. Cell culture flasks 75 cm².
15. Parafilm.
16. 24-well glass bottom plates such as ibidi μ -Plates (Ibidi, cat no. 82406) or Greiner Sensoplates (Greiner, cat. no. 662892).
17. Tissue culture incubator (37°C, 5% CO₂).
18. Benchtop centrifuge.
19. Haemocytometer.
20. Tissue culture microscope with 10x objective to count cells.
21. Neon Transfection System (ThermoFisher, cat. no. MPK5000).
22. Neon 100- μ L electroporation tips (ThermoFisher, cat. no. MPK10096).

23. Neon electroporation tube (ThermoFisher, cat. no. MPT100).
- 140 24. Neon E2 electrolytic buffer (ThermoFisher, cat. no. MPK10096).
25. Neon Buffer R (ThermoFisher, cat. no. MPK10096).
26. Arl13bCerulean-Fucci2a expressing Flp-In™ compatible pcDNA™5-CAG-Arl13bFucci2a plasmid: 1 µg/µL in TE (Ford et al 2018 - Riken BRC accession #RDB16057).
27. pOG44 Flp recombinase expressing plasmid: 1 µg/µL in TE (ThermoFisher, cat. no. 145 V600520).
28. pcDNA™5/FRT/CAT positive control plasmid: 1 ug/uL in TE (ThermoFisher, cat. no. V601020).

2.4. Confocal microscopy

1. Microscope: Laser scanning confocal platform (e.g. Nikon A1R) or spinning disc 150 confocal platform (e.g. Andor Dragonfly) (*see Note 2*).
2. Hardware autofocus (e.g. Nikon Perfect Focus System (PFS)) (*see Note 3*).
3. Environmental chamber to maintain a constant temperature of 37°C and deliver humidified 5% CO₂ to the sample (*see Note 4*).
4. Stage insert for microscope that accommodates multiwell plates.
- 155 5. High numerical aperture dry 20x or 40x objective for multiwell imaging (*see Note 5*).
6. Acquisition software (e.g. Nikon NIS Elements or Andor Fusion).

2.5. Image analysis

1. Fiji distribution of ImageJ.
- 160 2. Fucci_Tools.ijm macro toolset and fucci_tools_profile.txt (https://github.com/richiemort79/fucci_tools).

3. Methods

3.1. Generation of stable Arl13bCerulean-Fucci2a expressing cell lines

165 Given the toxicity of the Fucci2a probes when they are overexpressed and the variability in
expression levels generated between cells, transient transfection techniques are not
recommended when imaging Arl13bCerulean-Fucci2a. Therefore, we describe the generation of
a stable cell line using the Flp-In™ system (ThermoFisher). The Flp-In™ system allows the
integration of a single copy of a Flp-In™ compatible plasmid (harboring a single FRT site) into
170 the FRT site of a Flp-In™ locus in a compatible cell line (**Fig. 1D-E**). Integration of the plasmid
results in a switch of selection cassette allowing for selection of successful integrants.

1. Untargeted Flp-In™ NIH 3T3 cells (or other Flp-In™ compatible cells, *see Note 1*) are
maintained in culture media supplemented with 100 ng/mL Zeocin in 75 cm² flasks (*see*
175 **Note 6**). Approximately 1×10^7 cells are required for each transfection.
2. Prewarm 15 mL of Opti-MEM in 3 x 75 cm² tissue culture flasks.
3. Add 3 mL of electrolytic buffer E2 to the electroporation tube and insert into the Neon
pipette station.
4. Label three 1.5 mL tubes: negative control, positive control and Arl13bCerulean-Fucci2a.
180 Into each tube, pre-aliquot in 27 μ L of pOG44 plasmid. In the negative control tube, add
3 μ L TE. In the positive control tube, add 3 μ L pcDNA™5/FRT/CAT plasmid. In the
experimental tube, add 3 μ L of pcDNA™5-CAG-Arl13bFucci2a (*see Note 7*).
5. Wash the Flp-In™ cells with PBS, trypsinise, pellet in a 15 mL tube, wash with PBS and
count with a hemocytometer. Resuspend pellet in a volume of Neon Buffer R required
185 for the electroporation (i.e. aliquots of 5×10^7 cells each in 90 μ L Neon Buffer R, at a
final concentration of $\sim 5 \times 10^7$ cells/mL). For example, this workflow requires 9
aliquots total for the three conditions each requiring two experimental and one back-up
(*see Note 8*).
6. For each electroporation combine 10 μ L of the DNA from step four with one 90 μ L
190 aliquot of cells from step five. Use the Neon electroporation system (2 pulses: 1350 V, 20

ms for Flp-In™ 3T3) to electroporate the Flp-In™ cells. For each condition use 2 x 100 µL electroporations (use 1x 100 uL Neon tip twice per tube, change between conditions) and dispense both into the same 75 cm² flask containing pre-warmed Opti-MEM.

7. Place flasks in the incubator for 24 hours.

195 8. After 24 hours, remove the Opti-MEM and replace with 15 mL of culture media supplemented with 50 ng/mL Hygromycin B.

9. Grow cells under Hygromycin B selection changing the media every 3-4 days for 14 days and regularly inspect for clones.

200 10. Following 14 days of Hygromycin B selection or when well defined clonal colonies can be observed, trypsinise the cells and passage to generate a polyclonal Arl13bCerulean-Fucci2a expressing cell line. Using the the Flp-In™ system, generated cells are isogenic (i.e., integration occurs into the same genomic locus in every clone, such that all clones should be identical). This can be confirmed by determining loss of Zeocin-resistance, loss of lacZ expression as well as expression of Arl13bCerulean-Fucci2a biosensor
205 cassette.

11. Cryopreserve early passage cells in 1 mL aliquots of ~ 10⁶ cells/mL in freezing medium using 2 mL cryovials. Freeze cells following standard procedures and store long-term in liquid nitrogen.

210 3.2 Live cell imaging of Arl13bCerulean-Fucci2a expressing cells

Successful imaging of Arl13bCerulean-Fucci2a expressing cells requires striking a balance between image acquisition speeds, laser exposure and the number of parallel experiments one wishes to conduct. Consider the time it will take to image each position on the plate when deciding how many conditions to include in an experiment. When analyzing cilia and cell cycle
215 dynamics in parallel, we find it best to image each position every 10-20 minutes for 48-72 hours in order to capture multiple mitosis-to-mitosis transitions. However, catching rarer or transient events, such as decapitation, may require more frequent intervals, consequently decreasing the

number of parallel experiments or positions which can be imaged for each time point. We find that confocal systems that incorporate an environmental enclosure that encompasses the entire stage and that employ hardware autofocus are the most reliable for long term time-lapse because they are best at minimizing temperature variations as well as air currents or vibrations and therefore sample drift across long imaging sessions.

3.3. Experimental set-up

1. Wash the Flp-In™ Arl13bCerulean-Fucci2a cells with PBS, trypsinise, pellet in a 15 mL tube, wash with PBS and count with a hemocytometer.
2. Seed the cells into a 24-well glass bottomed plate containing imaging media in densities ranging from 1×10^5 to 5×10^5 cells per well (*see Note 9*). Use at least 1000 μ L media per well to account for evaporation across the imaging session. Incubate the plate for at least four hours prior to imaging to give the cells time to attach.
3. Fill the unused surrounding wells with 1000 μ L of sterile PBS to further minimize evaporation of the medium in adjacent wells.
4. If gassing with a needle, make a hole in the side of the 24-well plate with a hot hypodermic needle.
5. If not using a stage top enclosure, seal the outside of the plate with a strip of parafilm (*see Note 10*).
6. Pre-warm the environmental chamber and microscope stage for at least one hour prior to imaging to prevent stage drift.
7. Insert the glass bottomed 24-well plate into the microscope stage's plate insert and inside the chamber at 37°C, if gassing with a needle insert the needle into the hole in the plate.

3.4. Imaging set-up

- 245
1. Chose a lens- if acquiring data at multiple positions, dry lenses allow for ease of movement between positions over long time periods (*see Note 5*).
 2. In order to visualize Cerulean, Venus and Cherry, set the pinhole size according to the longest wavelength channel (Cherry) being recorded. This ensures that all channels have the same optical section thickness and that no channel has a pinhole size less than 1AU.
 - 250 3. For each channel, check pixel saturation and adjust to minimize over-saturation to keep in a dynamic range.
 4. To image multiple positions and/or wells, define the XY coordinates for each independent position using your imaging platform's acquisition software.
 5. We recommend including a small z-stack at each acquisition point to account for stage drift. This does not need to be the optimal "step size" calculated by the image
255 acquisition software, larger step sizes will increase the rate of acquisition and decrease the amount of light exposure to the sample. Capture a time series overnight at ~20-minute intervals for upwards of 48 hours in order to ensure that many complete mitoses are captured.

260 3.5. Image analysis with Fiji and Fucci Tools

ImageJ is a freeware image analysis platform based on NIH Image (Schneider et al 2012). Fiji is a distribution of ImageJ that includes many useful plugins and imaging libraries pre-installed (<https://fiji.sc/>) (Schindelin et al 2012). In order to investigate the dynamics of the cilia and cell cycles, the fluorescence intensity of the two Fucci2a probes must be monitored and
265 morphological measurements of the cilia must be made in parallel. We present "Fucci Tools" a macro toolset written for Fiji that allows users to manually track cell nuclei and cilia in order to capture this information. Fucci Tools allows for the easy tracking of the daughters of a cell division, summarizes the tracking data, fluorescence intensities and morphometric data in a comprehensive results table and allows plotting of the data in several useful formats. Substacks
270 cropped to the nucleus of interest are generated dynamically during tracking. The tracking data

can be parsed to the .mdf2 format allowing compatibility with MTrackJ, an ImageJ plugin to visualize and measure cell tracking statistics. Users can define an experimental profile that captures the key parameters from their image acquisition to streamline their workflow.

275 **3.6. Installation of Fucci_Tools.ijm and initial definition of an experimental profile**

Fucci Tools is free software provided under a Massachusetts Institute of Technology (MIT) license. Please read the license file included in the Fucci Tools GitHub repository. In order to help users set up and troubleshoot Fucci Tools, we have included the example dataset used in this chapter (Ford et al 2018), along with an example results table of tracking data that can be
280 imported to test the plotting functions.

1. Comprehensive instructions on the installation of Fiji can be found on the Fiji website (<https://fiji.sc/>).
2. Once Fiji has been successfully installed, download fucci_tools-master.zip from GitHub (https://github.com/richiemort79/fucci_tools) and extract the archive.
- 285 3. Place Fucci_Tools.ijm in the Fiji/macros/toolsets folder of your Fiji installation.
4. Place fucci_tools_profile.txt in the Fiji/macros folder of your Fiji installation. Restart Fiji.
5. Next define the image acquisition parameters that were used to capture the dataset. Open fucci_tools_profile.txt in a Text editor and edit the listed parameters (for an explanation *see Table 1*).

290

3.7. Performing an analysis with Fucci Tools.

1. Launch Fiji and open the dataset generated by your image acquisition software above. Fiji supports a wide number of proprietary image formats (*see Note 11*).
2. If a z-stack was captured during image acquisition, first flatten the data by either
295 selecting an individual z-plane for analysis or by using a maximum intensity projection.
3. On the main ImageJ toolbar click the “More Tools” menu button “>>” and select “Fucci Tools” from the drop-down menu.

- 300
4. Click the “Initialize” Tool (**Fig. 2 A-1**). The required parameters are loaded automatically from the `fucci_tools_profile.txt` file but can also be manually refined at this point. If you wish to track a cilium, remember to tick the “Track Cilia” checkbox in the initialize dialog.
 5. Scan through the time-lapse data to identify a cell that divides twice during the time lapse (*see Note 12*). Fucci Tools allows one to track the mother cell into the first division and then track both daughters. When a mother cell of interest has been identified click
305 the “Interactive Measure Tool” [2]. The tool button becomes greyed out when it is active.
 6. With “Interactive Measure Tool” (**Fig. 2 A-2**) selected click on the cell nucleus. A new track (Track 1) is added to the results table. The intensities of the individual channels will be recorded in the results table and a cropped version of the dataset will be recorded in the Substack window (**Fig 3C**).
 - 310 7. If “Track Cilia” was selected in the initialize dialog, Fucci Tools will prompt the user to make this measurement. Simply click “OK” in the dialog if no cilia are present at this time point otherwise use the “Segmented Line” tool to define the cilia. Double click to close the line and then press “OK” in the dialog window.
 8. The time lapse will then advance to the next frame so that the user can click and make
315 measurements again.
 9. At the point that the mother cell undergoes cytokinesis click the “Add Mitosis Tool” (**Fig. 2 A-4**) and then continue to track one of the daughters of the division. A new track (Track 1a) is added to the results table and a new Substack is opened.
 10. When the first daughter cell divides click the “Switch Daughter” tool (**Fig. 2 A-5**). This
320 will return the time lapse to the timepoint at which the mother underwent mitosis so that second daughter cell can be tracked. The mitosis point will be circled. A new track (Track 1b) is added to the results table and a new Substack is opened.
 11. At any time, a user can click the “Add Track Tool” (**Fig. 2 A-3**) to start tracking a new cell.

3.8. Plotting of the results table data

The manner in which one might plot the data generated by Fucci Tools will depend on the experimental question. However, we have included a number of plotting methods that will help in the initial exploration of datasets generated (Figs. 4 and 5, *see Note 13*). As well as the plotting functions described below, montages (Fig 5A) can be easily generated from the substacks collected during tracking (Fig. 3C) using standard ImageJ commands. Four types of plots are available in Fucci Tools: 1) "Single" plots of each complete mitosis (Fig. 5B) are generated either as a stack of images or as a montage (Fig. 4B). These plots included the normalized intensity of each channel chosen in the plot dialog (Fig. 4A) and an overlay that shows the normalized length of the cilia (if present) with time. Use these plots to examine how cilia assembly varies between individual cell cycles. 2) "Interpolated Mean" plots (Fig. 5 C) attempt to provide a method to examine the mean behavior of each probe across the length of a cell cycle. They are generated by interpolating the probe intensity and cilia length data using linear resampling so that a complete mitosis is represented by 100 arbitrary time-points. A mean and 95 % confidence interval is then generated for each fluorescent channel and for cilia length at each time point. 3) "Interpolated Fucci with Cilia Overlay" plots allow plotting of cilia assembly and disassembly times over mean fluorescence intensity plots (Fig. 5D). 4) In order to examine the heterogeneity in assembly and disassembly times, "Interpolated Cilia Length" plot trims the cilia length data to remove time points before assembly and after disassembly and then interpolates cilia length using linear resampling so that time is represented as 100 arbitrary points. A mean and 95 % confidence interval is then generated for cilia length at each timepoint. This allows examination of the mean behavior during cilia assembly maintenance and disassembly across all the tracks in the results table.

3.9. Concluding remarks

Careful observation at cellular and subcellular resolution with live imaging allows elucidation of the underlying intercellular heterogeneity of biological processes. Isogenic cell lines (or mouse tissues) expressing our Arl13bCerulean-Fucci2a biosensor allow users to capture a variety of cilia parameters in parallel to precise cell cycle stages. Here, we describe Fucci Tools, an analysis package, designed to enable users to easily elucidate multiple cilia and cell cycle parameters from imaging files and explore the data in a variety of informative formats. Fucci Tools allows examination of cilia assembly/disassembly and length mapped to a standardized cell cycle across many individual cells (**Fig. 5B-E**). We observe three phases in cilia dynamics during cell cycle progression: (1) fast assembly, with a heterogenous start time, up to ~50% of final length; (2) growth (+50% length) and maintenance until just before M phase; and (3) rapid disassembly at M-phase. We examined cell cycle progression times for adjacent cells in asynchronous cultures from two experiments to ask whether cell cycle times differ in ciliated cells (**Fig. 6**). While mean cell cycles varied between experiments (experiment A: ciliated = 37.7 ± 8.7 hr vs unciliated = 30.9 ± 8.1 hr; experiment B: ciliated = 44.1 ± 5.0 hr vs unciliated = 38.1 ± 9.0 hr, non-significant differences), it was intriguing that ciliated cells consistently took around 6 hours longer to divide (**Fig 6A**). When we asked what stage of the cycle they spent more time in, there was no clear trend (**Fig 6B**). In our analysis (**Fig 7**), we struggled to find many examples ($n = 1/25$ ciliated cells) of decapitation prior to cilia disassembly (Phua et al. 2017), but this could reflect differences operating in asynchronous cycling populations versus those stimulated by serum. It may also be possible that our time acquisition intervals are not frequent enough to capture these transient events. Adjusting image acquisition parameters to meet the requirements of your biological question is key to a successful experiment.

These tools will be important for comparing effects on cell cycle and cilia dynamics between genotypes, but also more fundamental questions. For example, how does a transient organelle which is required for mitogenic signals, like Hedgehog signaling, respond if it is only present for a portion of the cell cycle. Intriguing work from Ho, Tsai and Stearns using a medulloblastoma cell line, as well as cerebellar granular precursors cells from which they are

derived (Ho et al 2020), revealed that cilia also persisted into S phase where they mediate robust Hh signaling. If and how cilia content may change with the cell cycle is another open question-
380 with evidence suggesting this may be the case for phosphoinositide content (Phua et al 2017) and signaling competence in subsequent interphases (Ho et al 2020). Indeed, a recent study from the Mick lab, revealed specific and rapid remodeling of the cilia proteome in the timescale of 10s of minutes in response to Hh ligand (May et al 2020)- although how this occurred in the background of the cell cycle remains unclear. These observations raise questions as to the
385 physiological consequence of having a cilium at different stages of the cell cycle. Can they function as effective 'signaling organelles' if present regardless of cell cycle stage or are their contents and signaling competence regulated in a cell cycle specific manner? Our tools which allow simultaneous analysis of cell cycle stage, cilia kinetics and morphology provide a very powerful means to investigate these open questions.

390

4. Notes

1. It is also possible to use other Flp-In™ compatible cell lines, which for cilia research include RPE-1 Flp-In™ (Klebig et al 2009) or IMCD3 Flp-In™ (Mukhopadhyay et al 2010), as long as they include an FRT site integrated at a single genomic locus. Flp-In™ cell
395 lines can also be generated *de novo* by integration of the pFRT/lacZeo construct (ThermoFisher).
2. These require excitation and emission filters to allow imaging of Cerulean (433 nm/475 nm), Venus (515 nm/528 nm) and mCherry (587 nm/610nm) fluorescent proteins.
3. Hardware autofocus (i.e. Nikon's PFS) is highly advantageous for eliminating stage drift
400 especially in Z greatly reducing the number of failed multiday imaging experiments.
4. We have successfully used both microscope stage mounted systems that heat and provide CO₂ (e.g. Okolabs stage top incubator) and full environmental chambers that enclose the stage and objective lenses (e.g. Solent Scientific enclosures) in combination

- 405 with either CO₂ delivery by hypodermic needle to a parafilm sealed plate or using a passive Okolabs stage-top chamber for CO₂ delivery.
5. On most microscopes, multi-position acquisitions over long periods necessitate use of dry objectives as spreading of immersion media (oil or water) across the surface of a multi-well plate over time will interrupt focus of a high magnification lens. Some manufacturers like Leica offer a Water Immersion Micro Dispenser which overcomes
410 this potential problem during long-term live-cell imaging experiments like these. If using a dry 40x, check the correction collar is set for imaging through a standard #1.5 coverglass found on the bottom of Ibidi plates.
 6. It is imperative that Flp-In™ compatible cell lines are maintained during passaging according to the specific guidelines for retaining the FRT site integrated at a single
415 genomic locus. In the case of untargeted Flp-In™ NIH 3T3 cells, this requires culturing in culture media supplemented with 100 ng/ml Zeocin in order to retain ability to target efficiently.
 7. To avoid arcing, the total volume of DNA must not exceed 10% of the volume of cells. For transfection grade plasmid DNA, we recommend using commercial midi or maxi
420 DNA prep kits which allow elution in minimal volumes of endotoxin-free buffer.
 8. Pre-aliquoted plasmid reagents will help minimize the time cells spend in Neon Buffer R. A quick workflow to get cells back into medium is important for a successful transfection with optimal viability. When using the Neon transfection system, we recommend preparing transfections mixes (n+1), as cells can be quite viscous in Neon
425 Buffer R and there is a need to avoid bubbles taken up in the tip to avoid arcing (i.e. a spark). Discard cells if arcing occurs.
 9. Experiment with seeding density in order to get a density that allows easy tracking of cells. Especially for NIH 3T3 cells, we recommend plating at low density to allow imaging of exponentially growing cultures for tracking rates of ciliation in relation to

430 cell cycle. Moreover, some cell types including Flp-In™ 3T3 tend to migrate over one
another and can be hard to track. We find that mixing them 1:3-1:2 with unlabeled
parental cells can help with this.

10. Take care to avoid pulling the parafilm too tight as it may then fail overnight. Ensure no
parafilm underlaps the plate as this will prevent it from sitting flat on the microscope
435 stage.

11. Fiji comes with the Open Microscopy Environment (OME) Bio-formats plugins
(<https://www.openmicroscopy.org>) preinstalled. Bio-formats supports the opening of
many proprietary file types (e.g. Nikon .nd2, Zeiss .czi, Olympus .vsi) as
multidimensional 'Hyperstacks' in Fiji/ImageJ. If your Imaging format is not supported
440 export the data from your acquisition software as a .tif stack.

12. It is often easiest to scan backwards from the end of the time-lapse to identify cells to
track.

13. Whilst data from the three channels in the biosensors are associated with real spectra
and these are used for Fucci Tools, for accessible representation purposes we have
445 altered the use of 'false colour' in the 3 colour confocal images so that they are not red,
green and cyan but rather magenta, yellow and cyan. Similarly, we use this palette to
represent dynamics in our line art graphs too. These colour combinations that are more
favourably viewed by about 10% of the population who are red/green colour blind
(<https://imagej.nih.gov/ij/docs/guide/146-9.html> and [https://www.ascb.org/science-
450 news/how-to-make-scientific-figures-accessible-to-readers-with-color-blindness/](https://www.ascb.org/science-news/how-to-make-scientific-figures-accessible-to-readers-with-color-blindness/)).

455 **References**

1. Anderson CT, Stearns T (2009) Centriole age underlies asynchronous primary cilium growth in mammalian cells. *Curr Biol* 19:1498–1502. doi: 10.1016/j.cub.2009.07.034
- 460 2. Bernabé-Rubio M, Alonso MA (2017) Routes and machinery of primary cilium biogenesis. *Cell Mol Life Sci* 74:4077–4095. doi: 10.1007/s00018-017-2570-5
3. Ford MJ, Yeyati PL, Mali GR, Keighren MA, Waddell SH, Mjoseng HK, Douglas AT, Hall EA, Sakaue-Sawano A, Miyawaki A, Meehan RR, Boulter L, Jackson IJ, Mill P, Mort RL (2018) A Cell/Cilia Cycle Biosensor for Single-Cell Kinetics Reveals Persistence of Cilia after G1/S Transition Is a General Property in Cells and Mice. *Dev Cell* 47:509–465 523.e5. doi: 10.1016/j.devcel.2018.10.027
4. Garcia-Gonzalo FR, Reiter JF (2017) Open sesame: how transition fibers and the transition zone control ciliary composition. *Cold Spring Harb Perspect Biol* doi: 10.1101/cshperspect.a028134
- 470 5. Ho EK, Tsai AE, Stearns T (2020) Transient Primary Cilia Mediate Robust Hedgehog Pathway-Dependent Cell Cycle Control. *Curr Biol* 30:2829–2835.e5. doi: 10.1016/j.cub.2020.05.004
6. Ishikawa H, Marshall WF (2017) Intraflagellar transport and ciliary dynamics. *Cold Spring Harb Perspect Biol* doi: 10.1101/cshperspect.a021998
- 475 7. Klebig C, Korinth D, Meraldi P (2009) Bub1 regulates chromosome segregation in a kinetochore-independent manner. *J Cell Biol* 185:841–858. doi: 10.1083/jcb.200902128
8. May EA, Kalocsay M, Galtier D'Auriac I, Gygi SP, Nachury MV, Mick DU (2020) Time-resolved proteomic profiling of the ciliary Hedgehog response reveals that GPR161 and PKA undergo regulated co-exit from cilia. *BioRxiv* doi: 10.1101/2020.07.29.225797
- 480 9. Mirvis M, Siemers KA, Nelson WJ, Stearns TP (2019) Primary cilium loss in mammalian cells occurs predominantly by whole-cilium shedding. *PLoS Biol* 17:e3000381. doi: 10.1371/journal.pbio.3000381
10. Mort RL, Ford MJ, Sakaue-Sawano A, Lindstrom NO, Casadio A, Douglas AT, Keighren MA, Hohenstein P, Miyawaki A, Jackson IJ (2014) Fucci2a: a bicistronic cell cycle reporter that allows Cre mediated tissue specific expression in mice. *Cell Cycle* 13:2681–485 2696. doi: 10.4161/15384101.2015.945381
11. Mukhopadhyay S, Wen X, Chih B, Nelson CD, Lane WS, Scales SJ, Jackson PK (2010) TULP3 bridges the IFT-A complex and membrane phosphoinositides to promote trafficking of G protein-coupled receptors into primary cilia. *Genes Dev* 24:2180–2193. doi: 10.1101/gad.1966210
- 490 12. Paridaen JTML, Wilsch-Bräuninger M, Huttner WB (2013) Asymmetric inheritance of centrosome-associated primary cilium membrane directs ciliogenesis after cell division. *Cell* 155:333–344. doi: 10.1016/j.cell.2013.08.060

- 495 13. Phua SC, Chiba S, Suzuki M, Su E, Roberson EC, Pusapati GV, Schurmans S, Setou M, Rohatgi R, Reiter JF, Ikegami K, Inoue T (2017) Dynamic Remodeling of Membrane Composition Drives Cell Cycle through Primary Cilia Excision. *Cell* 168:264–279.e15. doi: 10.1016/j.cell.2016.12.032
14. Pugacheva EN, Jablonski SA, Hartman TR, Henske EP, Golemis EA (2007) HEF1-dependent Aurora A activation induces disassembly of the primary cilium. *Cell* 129:1351–1363. doi: 10.1016/j.cell.2007.04.035
- 500 15. Reiter JF, Leroux MR (2017) Genes and molecular pathways underpinning ciliopathies. *Nat Rev Mol Cell Biol* 18:533–547. doi: 10.1038/nrm.2017.60
16. Sakaue-Sawano A, Kurokawa H, Morimura T, Hanyu A, Hama H, Osawa H, Kashiwagi S, Fukami K, Miyata T, Miyoshi H, Imamura T, Ogawa M, Masai H, Miyawaki A (2008) Visualizing spatiotemporal dynamics of multicellular cell-cycle progression. *Cell* 132:487–498. doi: 10.1016/j.cell.2007.12.033
- 505 17. Schindelin J, Arganda-Carreras I, Frise E, Kaynig V, Longair M, Pietzsch T, Preibisch S, Rueden C, Saalfeld S, Schmid B, Tinevez J-Y, White DJ, Hartenstein V, Eliceiri K, Tomancak P, Cardona A (2012) Fiji: an open-source platform for biological-image analysis. *Nat Methods* 9:676–682. doi: 10.1038/nmeth.2019
- 510 18. Schneider CA, Rasband WS, Eliceiri KW (2012) NIH Image to ImageJ: 25 years of image analysis. *Nat Methods* 9:671–675. doi: 10.1038/nmeth.2089
19. Tucker RW, Scher CD, Stiles CD (1979) Centriole deciliation associated with the early response of 3T3 cells to growth factors but not to SV40. *Cell* 18:1065–1072. doi: 10.1016/0092-8674(79)90219-8
- 515 20. Wang L, Dynlacht BD (2018) The regulation of cilium assembly and disassembly in development and disease. *Development* doi: 10.1242/dev.151407

Acknowledgements

The authors are grateful to the IGMM Advanced Imaging Resource for imaging support and the BSCB for summer studentship support for MVK. PLY and PM were supported by core funding
520 from the UKRI Medical Research Council (MC_UU_00007/14). RLM was supported by funding from North West Cancer Research (CR1132) and the NC3Rs (#NC/T002328/1).

Figure Captions

Figure 1: Arl13bCerulean-Fucci2a - a tricistronic cell and cilia cycle biosensor. **A.** Schematic of the Arl13bCerulean-Fucci2a biosensor. A full-length mouse *Arl13b* cDNA was fused to the Cerulean fluorescent protein and concatenated to Fucci2a cell cycle probes hCdt1-mCherry and mVenus-hGem, with viral 2a peptide sequences in a multicistronic construct. **B.** Cell cycle phase specificity of the probes. mCherry abundance peaks in G1 and is lost at the G1/S transition, whereas mVenus is present through S/G2/M phases and is lost at mitosis. Primary cilia localization of ARL13B-Cerulean can be observed from G1 through S/G2 until M phase. (See **Note 13**). **C.** Asynchronous, Flp-In™ 3T3 cells stably expressing Arl13bCerulean-Fucci2a. **D.** The Flp-In™ system is used to make a single integration of the pcDNA5-CAG-Arl13bCerulean-Fucci2a plasmid into the genomic Flp-In™ locus of a compatible cell line. **E.** Integration of the plasmid switches the selection from Zeocin to Hygromycin. Scale bar in C = 100 μm.

Figure 2: Fucci Tools toolset and initialize dialog. **A:** The Fucci Tools appear in the main Fiji window as a toolset consisting of seven buttons. The function of which is as follows: 1) “Initialize Tool” to initialize the analysis and load the key parameters; 2) “Interactive Track Tool” for manually tracking cells; 3) “Add Track Tool ” to add a new track to the analysis; 4) “Add Mitosis Tool” to record mitotic events; 5) “Switch Daughter Tool” to record the end of a complete mitosis and return to its origin; 6) “Fucci Plot Tool” for plotting the acquired data; 7) “Parse to mdf2 Tool” to export the tracking data to MTrackJ for further analysis. **B:** The initialize dialog captures the key parameters for the analysis. Parameters are explained fully in Table 1. In order to track a cilium as well as analyzing the Fucci probe intensities, one must check “Track Cilia”, enter how often a cilium measurement is required to be made and which channels to view while measuring.

Figure 3. Fucci Tools toolbar and tracking features. **A:** ImageJ main window and Fucci Tools
550 toolset. **B:** A mitosis is tracked by following the mother followed by the two daughters the
positions of the nuclei in each frame are recorded and shown as an overlay (daughter a =
yellow, daughter b =red). **C:** Substacks of the nuclei are recorded for each track to make figure
preparation and data validation easier. **D:** A comprehensive tracking table is generated that
555 records the nuclei positions and fluorescence intensity in each channel as well as morphological
features of cilia. Scale bar In B = 100 μm , scale bar in C = 10 μm .

Figure 4: The Fucci Tools plotting dialog and montage view. **A:** The plotting dialog allows you
to check and amend acquisition parameters as well as choose the plot types you wish to
visualize. **B:** Selecting “Single” and “Montage” displays a montage of all the complete mitosis
560 tracks in the results table. Use the dialog to define the channels and features that you wish to
plot.

Figure 5: Advanced plotting of cilia and cell cycle dynamics. **A:** Substacks of a single
Arl13bCerulean-Fucci2a nucleus progressing through the cell and cilia cycles. **B:** Individual plot
565 showing normalized fluorescence intensity of the probes. The reciprocal mCherry-hCdt1
(magenta) and mVenus-hGem (yellow) Fucci2a peaks indicate the G1 and S/G2/M phases of
the cell cycle respectively. Normalized cilia length is indicated in cyan. **C:** Aggregated,
interpolated plot of n = 16 cell cycles. **D:** Aggregated Fucci2a intensities with cilia assembly and
disassembly times overlaid showing the diversity in assembly time with respect to cell cycle
570 phase. **E:** Aggregated plot of the normalized cilia plot across one cilia cycle. Error bars in B-D =
95% Confidence Intervals. Note: adjacent nuclei in A were masked for presentation purposes.
Abbreviations: A = ARL13B, C = hCdt1, G =hGem. Scale bar in A = 10 μm .

Figure 6: Cell cycle kinetics in adjacent ciliated versus unciliated cells. **A:** Total cell cycle
575 times (mitosis-to-mitosis) in hours (hr) from ciliated (cyan) versus unciliated (white) cells from
Analysis of cilia and cell cycle dynamics

two independent experiments. Mean and standard deviation (error bars) displayed. No significant difference between conditions (Student t-test, $P > 0.05$). Differences such as cell density between experiments may explain differences in cell cycle times. **B:** Individual proportions of cell cycle phases (G1: magenta vs S/G2/M: yellow) are represented grouped as ciliated versus unciliated cells. Mean proportion in G1 per cohort plotted as dotted black line. No significant difference between conditions (Student t-test $P > 0.05$). Abbreviations: Expt = experiment.

Figure 7: Ectocytosis/decapitation is a rare event in exponentially expanding cells. Out of the 25 ciliated full mitosis-to-mitosis events analyzed in these two data sets, only one decapitation event was observed. **A:** Montage at 60 minute timepoints reveals a cilium present from early in G1 through to just prior to nuclear envelope breakdown. **B:** At 20 minute timepoints the Ectocytosis event can be observed, the tip vesicle persisted for 2.2 hr. **C:** Individual plot showing normalised fluorescence intensity of the probes. Normalised cilia length is indicated in cyan. Decapitation occurred in G2, but cilia persisted for another 6.6 hr. Scale bar in A-B = 10 μm .

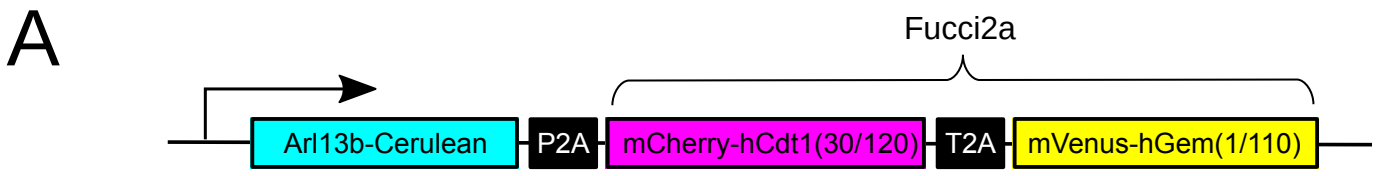
Table Captions

Table 1: Summary of the parameters defined by fucci_tools_profile.txt to establish an experimental profile. Use this file to define the key parameters used during image acquisition. These parameters will then be loaded automatically when Fucci Tools is initialized.

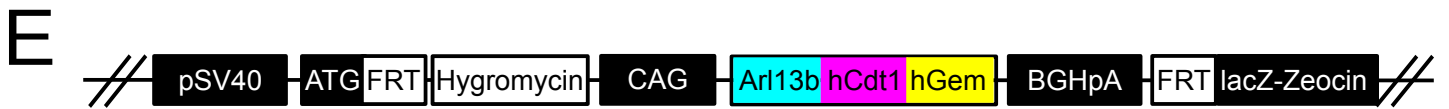
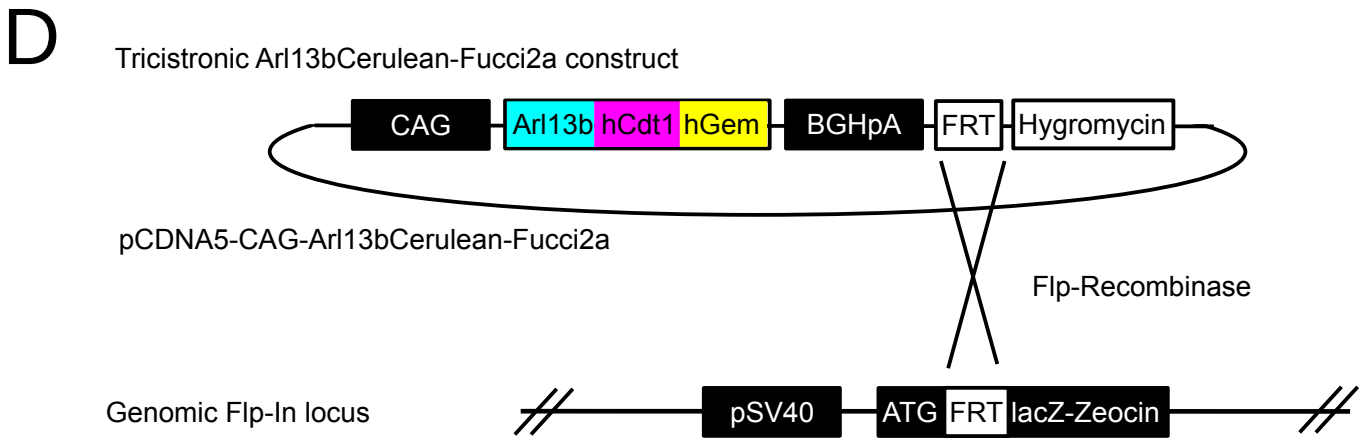
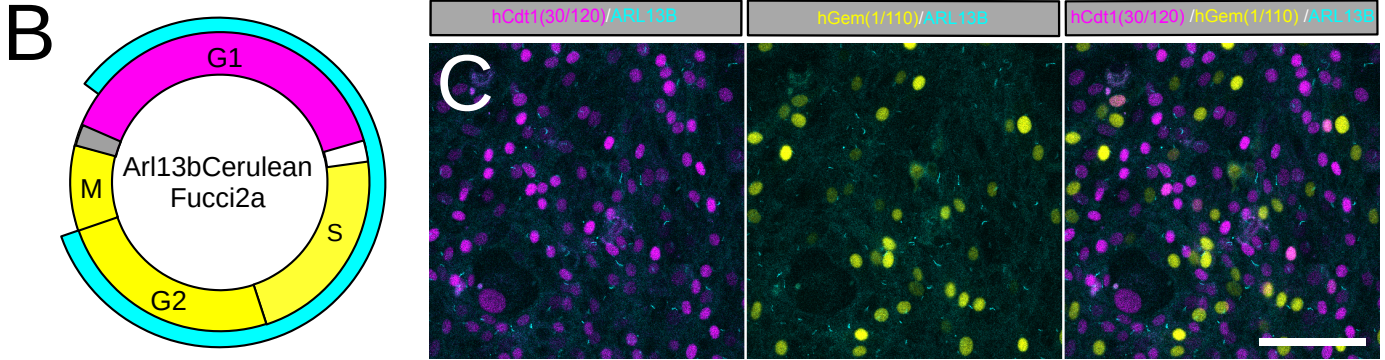
Table 1

Parameter	Description	Exempl
-----------	-------------	--------

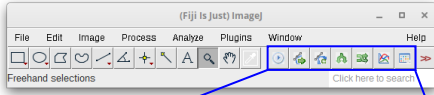
		e
pro_time_step	Time interval between frames in minutes	20
pro-scale	Image resolution in microns/pixel	0.42
pro_number_channels	Number of channels acquired in the dataset	4
pro_channels	The five available LUTS for visualization are: "Cyan,Green,Red,Magenta,Grays"	static
pro_channel_order	Map the above LUTS to the channels acquired in the dataset (1=Cyan, 2=Green, 3=Red, 4=Magenta, 5=Grays).	12304
pro_view	Define which channels are visible during the tracking analysis (1=visible, 0=hidden).	1110
pro_norm	Write 1 for channels for which the intensity values must be normalized for plotting, 0 if not	11111
pro-crop	Defines the dimensions of the required substack window in pixels.	50
pro_track	Write "true" if you would like to track and measure a cilium "false" if not.	true
pro_track_step	Define how often you would like to make measurements of the cilium (1 = measure every frame).	1
pro_view2	Define which channels are visible during the cilia analysis (1=visible, 0=hidden).	1000



Tricistronic Arl13bCerulean-Fucci2a construct

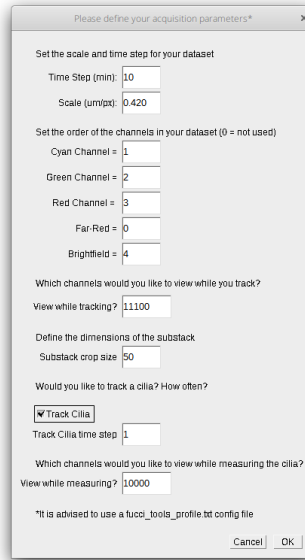


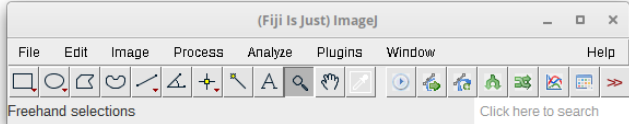
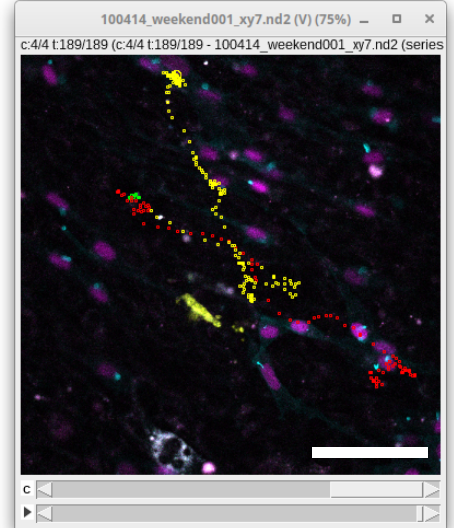
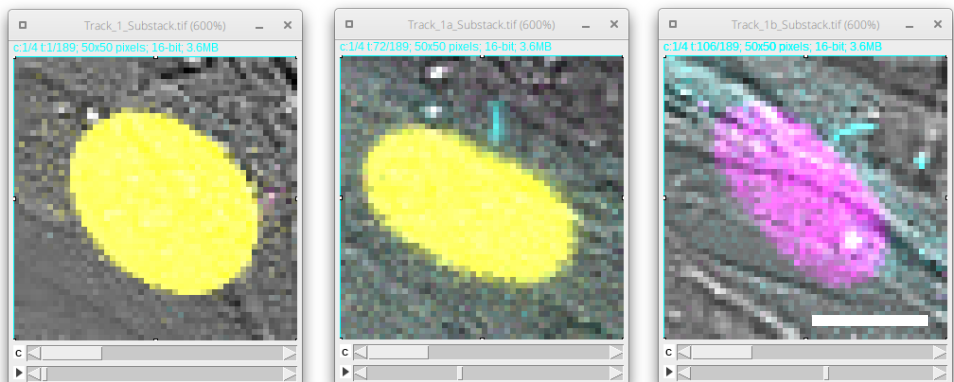
A



1 2 3 4 5 6 7

B



A**B****C**

Mother substack

Daughter 'a' substack

Daughter 'b' substack

D

100414_weekend001_xy7.nd2_Tracking Table

File	Edit	Font														
Image_ID	Track	Mother?	Frame	X	Y	Ch1_Mean	Ch2_Mean	Ch3_Mean	Ch4_Mean	Ch5_Mean	Cilia_COMX	Cilia_COMY	Distance_to_Cilia_(um)	Length		
1	280316_weekend_xy10.nd2	1	1	178	119	40.8000	1126.4000	22.3750	835.6000	0	188	116	10.4403	8.5440		
2	280316_weekend_xy10.nd2	1	2	178	122	38.2625	1232.4125	27.2000	799.8500	0	190	115	13.8924	7.2111		
3	280316_weekend_xy10.nd2	1	3	178	124	36.2500	1190.9875	21.1875	773.2375	0	190	124	12.0000	8.2462		
4	280316_weekend_xy10.nd2	1	4	183	124	43.5000	1260.1000	30.4375	796.2125	0	195	124	12.0000	6.7082		
5	280316_weekend_xy10.nd2	1	5	177	125	49.8125	1290.1500	29.7250	835.0125	0	190	125	13.0000	7.0711		
6	280316_weekend_xy10.nd2	1	6	181	124	85.7875	759.5750	26.6875	813.6125	0	190	128	9.8489	4.4721		
7	280316_weekend_xy10.nd2	1	7	180	118	45.9625	462.1875	34.5500	823.4375	0	180	117	1.0000	0.0000		
8	280316_weekend_xy10.nd2	1a	8	197	122	122.3125	88.1750	57.5625	739.0125	0	197	121	1.0000	0.0000		
9	280316_weekend_xy10.nd2	1a	9	196	126	68.8625	16.4500	72.0500	826.7625	0	196	125	1.0000	0.0000		
10	280316_weekend_xy10.nd2	1a	10	224	156	44.5625	18.4625	70.7125	828.6500	0	224	155	1.0000	0.0000		
11	280316_weekend_xy10.nd2	1a	11	230	167	74.5875	27.3125	89.6250	784.6000	0	230	166	1.0000	0.0000		
12	280316_weekend_xy10.nd2	1a	12	193	131	46.2625	21.1500	110.6250	773.5625	0	193	130	1.0000	0.0000		
13	280316_weekend_xy10.nd2	1a	13	194	133	54.5125	26.1000	135.1750	781.6125	0	194	132	1.0000	0.0000		
14	280316_weekend_xy10.nd2	1a	14	193	128	70.1250	24.3500	146.6500	760.5250	0	193	127	1.0000	0.0000		
15	280316_weekend_xy10.nd2	1a	15	191	128	48.3375	28.6875	208.1375	701.7875	0	191	127	1.0000	0.0000		
16	280316_weekend_xy10.nd2	1a	16	191	129	45.6875	30.8000	233.8500	747.2375	0	191	128	1.0000	0.0000		
17	280316_weekend_xy10.nd2	1a	17	191	136	57.8750	37.2625	274.9000	837.3125	0	191	135	1.0000	0.0000		
18	280316_weekend_xy10.nd2	1a	18	188	140	94.6125	34.3250	301.9625	838.6125	0	188	139	1.0000	0.0000		

A

Plotting parameters

Time Step (min): 10

Cyan Channel = 1

Green Channel = 2

Red Channel = 3

Far-Red = 4

Brightfield = 5

Print to Log?

Choose the features you wish to plot:

Cyan Green

Red Magenta

Grays Cilia Length

Choose the plot types you wish to see:

Single

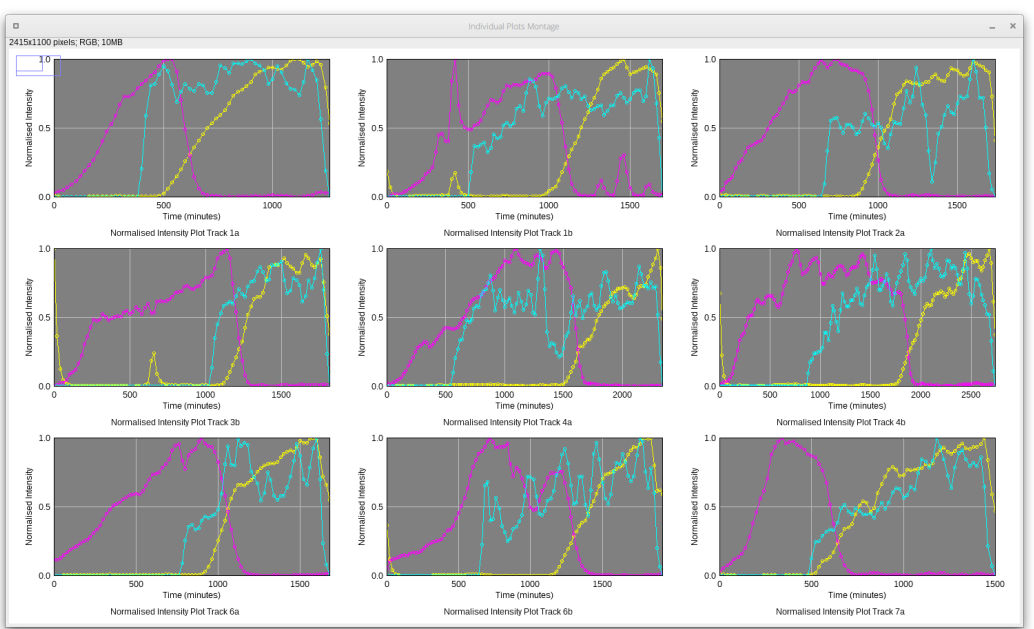
Montage

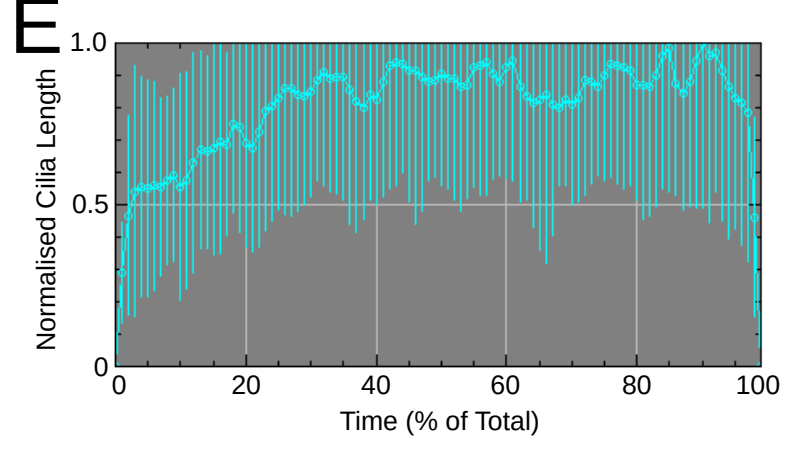
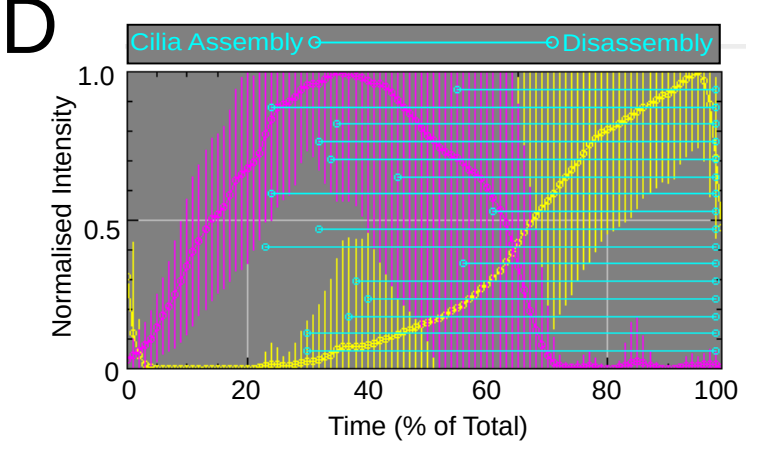
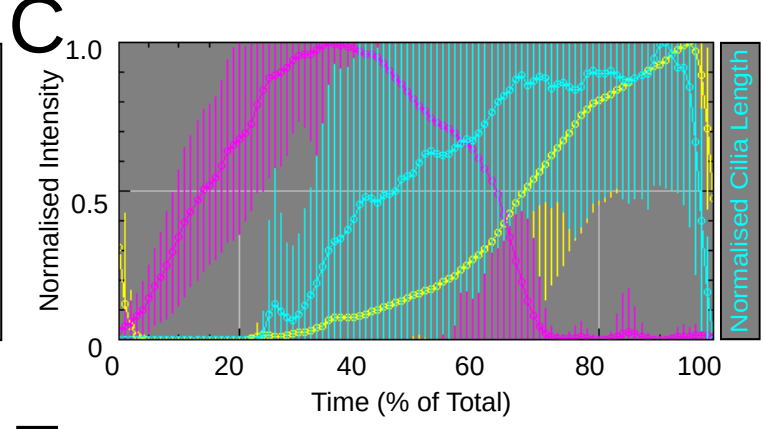
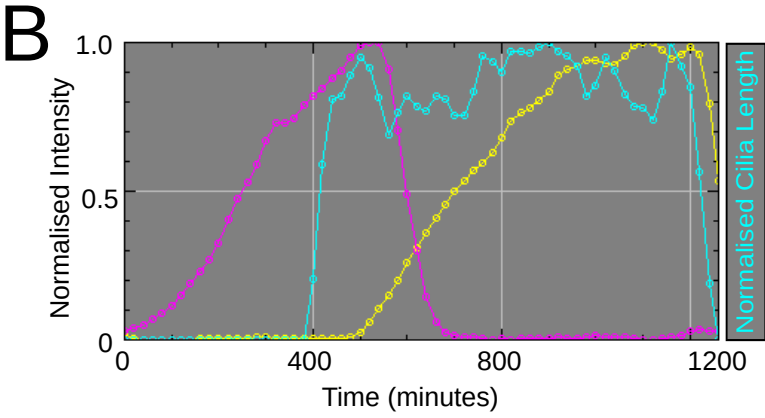
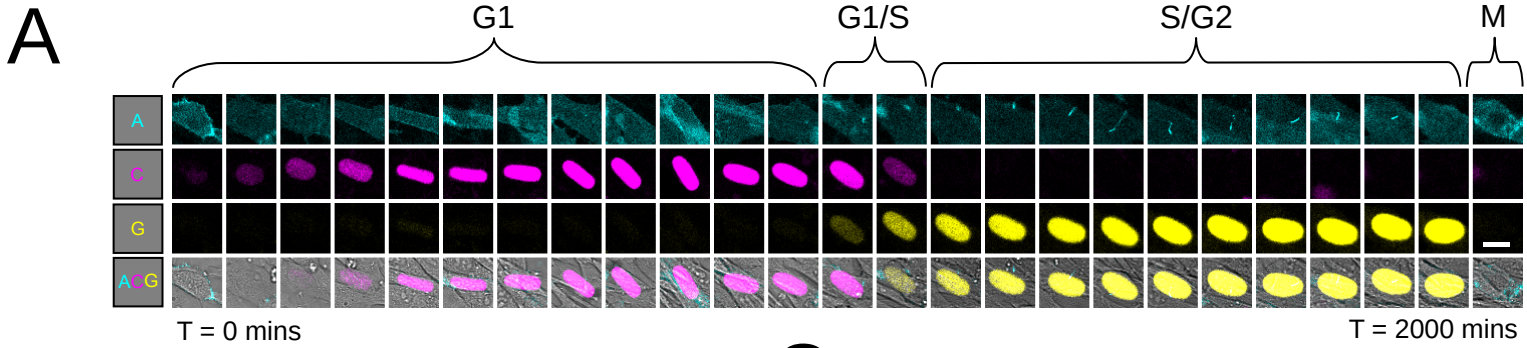
Interpolated Mean

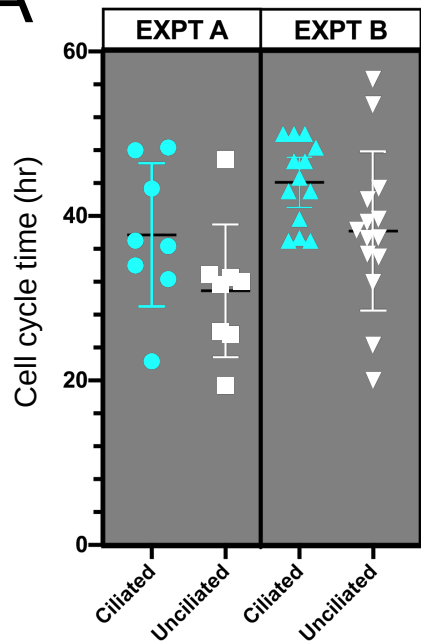
Interpolated Cilia Length

Interpolated Fucci with Cilia Overlay

Cancel OK

B



A**B**